

Five-component model validation of reference, laboratory and field methods of body composition assessment

Grant M. Tinsley*

Energy Balance & Body Composition Laboratory, Department of Kinesiology & Sport Management, Texas Tech University, Lubbock, TX 79409, USA

(Submitted 23 June 2020 – Final revision received 14 August 2020 – Accepted 3 September 2020 – First published online 14 September 2020)

Abstract

This study reports the validity of body fat percentage (BF%) estimates from several commonly employed techniques as compared with a five-component (5C) model criterion. Healthy adults (n 170) were assessed by dual-energy X-ray absorptiometry (DXA), air displacement plethysmography (ADP), multiple bioimpedance techniques and optical scanning. Output was also used to produce a criterion 5C model, multiple variants of three- and four-component models (3C; 4C) and anthropometry-based BF% estimates. Linear regression, Bland–Altman analysis and equivalence testing were performed alongside evaluation of the constant error (CE), total error (TE), SE of the estimate (SEE) and coefficient of determination (R^2). The major findings were (1) differences between 5C, 4C and 3C models utilising the same body volume (BV) and total body water (TBW) estimates are negligible (CE \leq 0.2%; SEE $<$ 0.5%; TE \leq 0.5%; R^2 1.00; 95% limits of agreement (LOA) \leq 0.9%); (2) moderate errors from alternate TBW or BV estimates in multi-component models were observed (CE \leq 1.3%; SEE \leq 2.1%; TE \leq 2.2%; $R^2 \geq$ 0.95; 95% LOA \leq 4.2%); (3) small differences between alternate DXA (i.e. tissue $v.$ region) and ADP (i.e. Siri $v.$ Brozek equations) estimates were observed, and both techniques generally performed well (CE $<$ 3.0%; SEE \leq 2.3%; TE \leq 3.6%; $R^2 \geq$ 0.88; 95% LOA \leq 4.8%); (4) bioimpedance technologies performed well but exhibited larger individual-level errors (CE $<$ 1.0%; SEE \leq 3.1%; TE \leq 3.3%; $R^2 \geq$ 0.94; 95% LOA \leq 6.2%) and (5) anthropometric equations generally performed poorly (CE 0.6–5.7%; SEE \leq 5.1%; TE \leq 7.4%; $R^2 \geq$ 0.67; 95% LOA \leq 10.6%). Collectively, the data presented in this manuscript can aid researchers and clinicians in selecting an appropriate body composition assessment method and understanding the associated errors when compared with a reference multi-component model.

Key words: Multi-component models: Multi-compartment models: Dual-energy X-ray absorptiometry: Air displacement plethysmography: Bioimpedance: Anthropometry

The importance of body composition in health and disease is well established^(1–4). However, contemporary methods of body composition estimation vary widely in their precision, accuracy and overall utility⁽⁵⁾. The variable performance of techniques is confounded by dissimilarities in ‘reference’ methods and differing interpretations of acceptable agreement. Indeed, the utilisation of dual-energy X-ray absorptiometry (DXA) and other non-criterion laboratory methods for validation or calibration of simpler body composition methods has been identified as a noteworthy challenge to the clear establishment of acceptable whole-body methods^(6,7). However, while some methodological questions remain unresolved, a relative consensus exists that multi-component models are true *in vivo* reference methods for estimation of total body composition at the molecular level^(6,8).

Molecular-level multi-component models (i.e. multi-compartment models) separate all body mass (BM) into three or more components and typically require assessments using multiple laboratory techniques. Using specific input variables, most commonly the mass, volume, water content and bone mineral of the body, whole-body fat and fat-free mass (FFM) can be estimated using validated equations⁽⁶⁾. Several decades ago, it was established that multi-component models containing estimates of the body’s mass, volume and water content demonstrated the highest validity as compared with a criterion six-compartment model produced independently using *in vivo* neutron activation analysis⁽⁷⁾. Consequently, based on the inaccessibility of neutron activation facilities, it was suggested that the validated molecular-level multi-component models be used as reference methods in future work^(6,9). While some investigations have appropriately employed these models as reference methods,

Abbreviations: ADP, air displacement plethysmography; BF%, body fat percentage; BIS, bioimpedance spectroscopy; BV, body volume; CE, constant error; DoD, Department of Defense; DXA, dual-energy X-ray absorptiometry; FFM, fat-free mass; LOA, limits of agreement; NHANES, National Health and Nutrition Examination Survey; SEE, standard error of the estimate; SFBIA, single-frequency bioelectrical impedance analysis; TBW, total body water; TE, total error.

* **Corresponding author:** Grant M. Tinsley, email grant.tinsley@ttu.edu

many contemporary technologies have limited or no validity data using a multi-component model reference method^(5,6,10).

Traditionally, the utilisation of multi-component models has been limited by the requisite time, expense and expertise. However, two developments have increased the accessibility of these models. First, the validation of specific bioimpedance techniques against dilution reference methods for the estimation of total body water (TBW) has allowed for removal of the most time-intensive component of traditional multi-component models^(11–15). More recently, the utilisation of DXA-derived body volumes (BV) has allowed for a 'rapid' four-component (4C) model using only BM estimates, a DXA scan and a simple bioelectrical impedance assessment^(16–18). While the utilisation of bioimpedance techniques is generally viewed as acceptable, particularly given the grossly disparate time required for assessment of TBW via dilution (hours for collection, followed by subsequent laboratory analysis) as compared with bioimpedance (minutes, with data immediately available), the utilisation of DXA-derived BV is less established, although a growing number of researchers have examined its use within a rapid 4C model^(16–23).

While several common body composition assessment techniques have been evaluated in comparison with multi-component models^(10,13,24,25), the wide heterogeneity of specific devices and persistent technological improvement necessitate continued investigation of these frequently employed methods. Based on the continued need for multi-component model validation of laboratory and field body composition assessment techniques, the purpose of the present investigation was to determine the validity of body fat percentage (BF%) estimates from a variety of commonly employed methods, ranging from simple anthropometric equations to modified multi-component models, as compared with a five-component (5C) model criterion. BF% was selected as the body composition outcome of interest due to its applicability across the full spectrum of body sizes.

Methods

Overview

After an overnight food and fluid fast, 170 healthy adults were assessed by DXA, air displacement plethysmography (ADP), bioimpedance spectroscopy (BIS), multi-frequency bioelectrical impedance analysis (MFBIA), single-frequency bioelectrical impedance analysis (SFBIA) and three-dimensional optical scanning. In addition to providing BF% estimates, output from these techniques was used to produce a reference 5C model and multiple variants of 4C and three-component (3C) models. Circumferences from optical scanning were used in anthropometric BF% equations from the USA Department of Defense (DoD) as well as newer equations developed using National Health and Nutrition Examination Survey (NHANES) data. All BF% estimates were compared with the 5C model, and relevant group- and individual-level error metrics were generated.

Participants

Adults from the general population were recruited for participation. Prospective participants were excluded if they were <18 or >75 years of age, weighed >159 kg or were >193 cm in height (due to limitations of the DXA scanner), were missing any limbs or parts of limbs, had a pacemaker or electrical implant, had implanted metal due to prior medical procedure, were currently pregnant or trying to become pregnant or had previously undergone a body-altering surgery (e.g. breast augmentation, liposuction). One hundred and seventy participants completed the study and were included in the present analysis (Table 1). This study was conducted according to the guidelines laid down in the Declaration of Helsinki, and all procedures involving human participants were approved by the Texas Tech University institutional review board (IRB2018-417). Written informed consent was obtained from all participants.

Laboratory assessments

Initial procedures. Participants reported to the laboratory wearing light athletic clothing after overnight (≥8 h) abstinence from eating, drinking, exercising and ingesting alcohol or caffeine. Adherence to these procedures was confirmed via interview. Prior to testing, all metal and accessories were removed, and each participant voided his or her bladder. Urine samples were collected, and urine specific gravity was assessed using a digital refractometer (PA201X-093, Misco). Equipment was calibrated as recommended by device manufacturers each day prior to use.

Dual-energy X-ray absorptiometry. DXA scans were performed on a Lunar Prodigy scanner (General Electric) with enCORE software (version 16.2). The scanner was calibrated daily prior to scanning using a manufacturer-supplied calibration block. Positioning of participants took place using custom-made foam blocks in order to promote consistency of positioning^(26,27). Foam blocks were placed bilaterally between the hands and hips, with the hands placed in a neutral position. A block and strap at the feet ensured consistent foot positioning and orientation of the feet perpendicular to the scanning table. In the event that a participant was too broad to fit within DXA's scanning dimensions, excluded body portions were estimated via reflection scanning techniques, which introduce minimal error^(28,29). A trained operator manually adjusted region of interest lines within the enCORE software to specify body segments (i.e. arms, trunk and legs). DXA estimates of tissue and region BF% were obtained. DXA bone mineral content was multiplied by 1.0436 to yield an estimate of bone mineral (Mo)^(6,7). DXA estimates of lean soft tissue, fat mass and bone mineral content were also utilised to predict an additional BV estimate for use in a rapid 4C model using equation (1), which was developed by Wilson *et al.*⁽¹⁸⁾ for GE DXA scanners:

$$BV(L) = 0.933 \times LST + 1.150 \times FM + -0.438 \times BMC + 1.504 \quad (1)$$

Air displacement plethysmography. ADP (BOD POD®, Cosmed USA) was performed according to manufacturer





Table 1. Participant characteristics (Mean values and standard deviations; numbers)

	All (n 170)		F (n 95)		M (n 75)	
	Mean	SD	Mean	SD	Mean	SD
Descriptive characteristics						
Age (years)	33.2	15.2	33.0	15.9	33.5	14.2
Body mass (kg)	73.4	16.4	65.0	12.0	84.0	15.2
Height (cm)	171.3	9.3	165.2	6.0	178.9	6.6
BMI (kg/m ²)	24.9	4.3	23.8	4.1	26.2	4.3
USG	1.021	0.008	1.021	0.009	1.021	0.007
FFM characteristics*						
D _{FFM} (g/cm ³)	1.097	0.009	1.097	0.009	1.096	0.008
TBW:FFM (%)	73.5	2.4	73.6	2.5	73.4	2.4
M:FFM (%)	6.3	0.5	6.4	0.5	6.1	0.4
R:FFM (%)	20.2	2.3	20.0	2.3	20.5	2.3
5C model components						
M _{FAT} (kg)	19.5	9.1	20.3	8.1	18.4	10.1
M _{TBW} (kg)	39.7	9.5	33.0	4.8	48.2	6.7
M _{Mo} (kg)	2.9	0.6	2.4	0.3	3.4	0.5
M _{Ms} (kg)	0.5	0.1	0.4	0.1	0.6	0.1
M _R (kg)	10.9	2.8	8.9	1.4	13.4	2.1
Residual components†						
M _{PRO} (kg)	10.4	2.7	8.6	1.4	12.9	2.1
M _G (kg)	0.5	0.1	0.4	0.1	0.6	0.1
Race/ethnicity (n)						
Caucasian (Non-Hispanic)	120		65		55	
Caucasian (Hispanic)	26		18		8	
Black/African American	16		6		10	
Asian	8		6		2	

F, female; M, male; USG, urine specific gravity; FFM, fat-free mass; D_{FFM}, density of fat-free mass; TBW:FFM, total body water to fat-free mass ratio; M:FFM, mineral (M_o + M_s) to fat-free mass ratio; R:FFM, residual to fat-free mass ratio; 5C, five-component model; M_{FAT}, fat mass; M_{TBW}, total body water mass; M_{Mo}, bone mineral mass; M_{Ms}, soft tissue mineral mass; M_R, residual (protein + glycogen) mass; M_{PRO}, protein mass; M_G, glycogen mass.

* Reference values based on direct cadaver analysis are⁽⁵²⁾: D_{FFM} = 1.099 (SD 0.015); TBW:FFM = 73.7 (SD 3.8) %; M:FFM = 6.6 (SD 0.8) %; R:FFM = 19.7 (SD 3.2) %.

† Residual mass (M_R) can further be divided into protein mass (M_{PRO}) and glycogen mass (M_G) in order to generate a six-component model using the assumption that M_R = M_{PRO} + M_G, alongside the equation of Wang as presented by Heymsfield⁽⁶⁾: M_G = 0.044 × M_{PRO}.

recommendations and included two to three volume measurements to ensure consistent values. Measured thoracic gas volumes were used. ADP has previously demonstrated similar body density (*D_b*) values to hydrostatic weighing and is considered a valid volumetric estimation technique for use in multi-component models^(24,30,31). Additionally, BF% estimates were obtained from ADP using the Siri⁽³²⁾ (equation (2)) and Brozek⁽³³⁾ (equation (3)) equations:

$$BF\% = \left[\left(\frac{4.95}{D_b} \right) - 4.5 \right] \times 100 \quad (2)$$

$$BF\% = \left[\left(\frac{4.57}{D_b} \right) - 4.142 \right] \times 100 \quad (3)$$

The same *D_b* value was used in both equations to yield two separate ADP BF% estimates for all participants, with the exception of Black/African American males (*n* 10) and females (*n* 6), who were evaluated using the equations of Schutte⁽³⁴⁾ and Ortiz⁽³⁵⁾, respectively, as recommended by the manufacturer. For these individuals, the estimates obtained by the Schutte and Ortiz equations were used for both ADP BF% estimates. However, for conciseness, the ADP BF% estimates in this investigation are referred to as ‘Siri’ and ‘Brozek’ since the large majority of individuals (>90 %) were assessed using these equations.

Bioimpedance spectroscopy. BIS (SFB7, ImpediMed) was utilised to obtain TBW estimates using the manufacturer-specified hand-to-foot electrode arrangement. Each participant remained supine for ≥3 min immediately prior to BIS assessment. Coefficients utilised for males ($\rho_e = 273.9$, $\rho_i = 937.2$) and females ($\rho_e = 235.5$, $\rho_i = 894.2$), as well as body density, body proportion and hydration values (1.05, 4.30 and 0.732, respectively) were the same as those utilised in previous investigations with the selected BIS analyser^(36–38). The BIS analyser used in the present study has previously been validated against deuterium dilution^(36,37) and obtains TBW estimates through Cole modelling⁽³⁹⁾ and mixture theories⁽⁴⁰⁾ rather than regression equations used by the majority of bioimpedance methods (e.g. BIA)⁽¹²⁾. BIS TBW volume estimates have compared favourably with dilution techniques in prior validation work^(14,15). In the present study, assessments were conducted in duplicate and averaged for analysis. BIS output was reviewed for quality assurance through visual inspection of Cole plots. BIS TBW was also utilised for prediction of soft tissue mineral (M_s) using equation (4), which was developed by Wang *et al.*⁽⁴¹⁾ using delayed-*Y* *in vivo* neutron activation:

$$M_s = 0.882 \times (12.9 \times TBW) + 37.9 \quad (4)$$

Multi-frequency bioelectrical impedance analysis. Multi-frequency bioelectrical impedance analysis was performed

using a 19-frequency, eight-point device (mBCA 515/514, Seca® GmbH & Co.) with contact electrodes and assessments conducted in the standing position. This analyser utilises frequencies ranging from 1 to 1000 kHz, a measuring current of 100 µA and has previously been validated against a 4C model for body composition estimates^(42,43). Assessments were conducted in duplicate and averaged for analysis.

Single-frequency bioelectrical impedance analysis. The SFBIA analyser (Quantum V, RJL Systems) was tested daily before any measurements using a manufacturer-supplied testing cell. Participant assessments were performed after approximately 5 min of supine rest. The SFBIA analyser employed an eight-point, bilateral, hand-to-foot electrode configuration. Electrode sites on the hand/wrist and foot/ankle were cleaned with alcohol pads prior to placement of the manufacturer-supplied adhesive electrodes. Electrodes were placed on the dorsal surfaces of both hands and both feet according to manufacturer specifications. Prior to assessment, each participant's limbs were spread apart to ensure that they did not contact other body regions. Participants remained motionless in the supine position during assessments, and bioelectrical output was processed using manufacturer-provided software (RJL BC Segmental version 1.1.2). Assessments were conducted in duplicate and averaged for analysis.

Three-dimensional optical imaging. Three-dimensional optical imaging was performed using a structured light scanner with static components (Size Stream® SS20; scanner version 6.0.0.32)⁽⁴⁴⁾. This scanner utilises a reference object, in the form of a hanging panel with checkerboard pattern, for sensor calibration prior to scanning. The calibration procedure was completed daily prior to scanning. Participants wore minimal form-fitting clothing during assessments. Scans were conducted in duplicate using a five-scan multi-scan mode and averaged for analysis. Scans were processed using Size Stream Studio software version 5.2.7 to obtain height and circumference estimates used in the anthropometric BF% equations. The root mean square coefficient of variation and intraclass correlation coefficient for height estimates in our laboratory, using the three-dimensional optical scanner, are 0.22 and 0.998 %, respectively. The reliability of other anthropometric estimates from this scanner has previously been reported⁽⁴⁴⁾.

Multi-component models

The criterion estimate of body composition was obtained from a 5C model (Table 2). In this model, BV was obtained from ADP, Mo from DXA and TBW and M_s from BIS. The BM estimate was obtained from the calibrated scale associated with the ADP device.

The equation of Wang *et al.*⁽⁴¹⁾ (equation (5)) was utilised for estimation of 5C BF%:

$$\text{BF\%} = 100 \times \frac{2.748 \times \text{BV} - 0.715 \times \text{TBW} + 1.129 \times \text{Mo} + 1.222 \times M_s - 2.051 \times \text{BM}}{\text{BM}} \quad (5)$$

Additional multi-component models estimates were produced. The Wang *et al.*⁽⁴¹⁾ 4C estimate was produced using equation (6):

$$\text{BF\%} = 100 \times \frac{2.748 \times \text{BV} - 0.699 \times \text{TBW} + 1.129 \times \text{Mo} - 2.051 \times \text{BM}}{\text{BM}} \quad (6)$$

Versions of the Wang *et al.* 4C model were produced using BIS, multi-frequency bioelectrical impedance analysis and SFBIA TBW estimates. An additional model, the rapid 4C model, was produced using the DXA-derived BV estimate.

The Siri three-compartment (3C) model was calculated using equation (7), as presented in Siri⁽⁴⁵⁾:

$$\text{BF\%} = 100 \times \left(\frac{2.118}{D_b} - 0.78 \frac{\text{TBW}}{\text{BM}} - 1.354 \right) \quad (7)$$

D_b estimates were obtained from ADP, and BIS TBW was used. Alternate versions of the Siri 3C model were produced using multi-frequency bioelectrical impedance analysis and SFBIA TBW.

Additionally, the Lohman 3C model⁽⁴⁶⁾, which includes an estimate of total body mineral (M; equivalent to $\text{Mo} \times 1.235$ ⁽⁴⁷⁾), was calculated using equation (8):

$$\text{BF\%} = 100 \times \frac{6.386 \times \text{BV} + 3.96 \times \text{M} - 6.09 \times \text{BM}}{\text{BM}} \quad (8)$$

Anthropometric body composition equations

Anthropometric BF% estimations were calculated using the Department of Defense (DoD)/army body fat equations⁽⁴⁸⁾, and three equations developed using National Health and Nutrition Examination Survey (NHANES) data by Lee *et al.*⁽⁴⁹⁾. These equations were developed using manual circumferences obtained with a tape measure. In the present investigation, the anthropometric estimates from three-dimensional optical imaging were utilised⁽⁴⁴⁾. Previous research has indicated that circumference estimates obtained by three-dimensional optical scanning may exhibit either slightly superior⁽⁵⁰⁾ or inferior⁽⁵¹⁾ reliability as compared with manual estimates, which may depend on the expertise of the manual assessor.

The DoD BF% equations for females (equation (9)) and males (equation (10)) are⁽⁴⁸⁾

$$\text{BF\%} = (163.205 \times \log_{10}(\text{WC} + \text{HC} - \text{NC})) - (97.684 \times \log_{10}(\text{height})) - 78.387 \quad (9)$$

$$\text{BF\%} = (86.010 \times \log_{10}(\text{WC} - \text{NC})) - (70.041 \times \log_{10}(\text{height})) + 36.76 \quad (10)$$

In these equations, WC refers to waist circumference, HC is hip circumference and NC is neck circumference, with all values entered in inches.

Several progressively more complex equations were produced from NHANES data by Lee *et al.*⁽⁴⁹⁾. For equations (11–16), additional terms for race/ethnicity adjustments were included using the appropriate coefficients presented in Table 2 of Lee *et al.*⁽⁴⁹⁾. For females, the equations developed by Lee *et al.*, which correspond to equations 1–3 in the original report⁽⁴⁹⁾, are



Table 2. Description of body composition models

Model	BM	BV	TBW	Mo	Ms	Overlap with 5C
5C	CS	ADP	BIS	DXA	BIS	–
4C	CS	ADP	BIS	DXA	–	BM, BV, TBW, Mo
4C _{MFBIA}	CS	ADP	MFBIA	DXA	–	BM, BV, Mo
4C _{SFBIA}	CS	ADP	SFBIA	DXA	–	BM, BV, Mo
4C _{DXA}	CS	DXA	BIS	DXA	–	BM, TBW, Mo
3C	CS	ADP	BIS	–	–	BM, BV, TBW
3C _{MFBIA}	CS	ADP	MFBIA	–	–	BM, BV
3C _{SFBIA}	CS	ADP	SFBIA	–	–	BM, BV
3C _{LOHMAN}	CS	ADP	–	DXA	–	BM, BV, Mo
DXA _{REG}	DXA	–	–	DXA	–	Mo
DXA _{TISS}	DXA	–	–	–	–	–
ADP _{BROZEK}	CS	ADP	–	–	–	BM, BV
ADP _{SIRI}	CS	ADP	–	–	–	BM, BV
BIS	CS	–	BIS	–	–	BM, TBW
MFBIA	S	–	MFBIA	–	–	–
SFBIA	CS	–	SFBIA	–	–	BM
DoD	–	–	–	–	–	–
LEE _{EQ1}	CS	–	–	–	–	BM
LEE _{EQ2}	CS	–	–	–	–	BM
LEE _{EQ3}	CS	–	–	–	–	BM

BM, body mass; BV, body volume; TBW, total body water; Mo, bone mineral; Ms, soft tissue mineral; 5C, five-component model; CS, calibrated scale; ADP, air displacement plethysmography; BIS, bioimpedance spectroscopy; DXA, dual-energy X-ray absorptiometry; 4C, four-component model; MFBIA, multi-frequency bioelectrical impedance analysis; SFBIA, single-frequency bioelectrical impedance analysis; 3C, three-component model; REG, region; TISS, tissue; BROZEK, Brozek⁽³³⁾ two-component model body fat equation; SIRI, Siri⁽³²⁾ two-component model body fat equation; S, scale built into MFBIA analyzer; DoD, Department of Defense body fat equation⁽⁴⁸⁾; LEE, Lee *et al.*⁽⁴⁹⁾ body fat equations.

$$BF\% = 58.60 + 0.08 \times \text{age} - 0.30 \times \text{height} + 0.35 \times BM \quad (11)$$

$$BF\% = 50.46 + 0.07 \times \text{age} - 0.26 \times \text{height} + 0.27 \times BM + 0.10 \times WC \quad (12)$$

$$BF\% = 27.57 + 0.08 \times \text{age} - 0.17 \times \text{height} + 0.09 \times BM + 0.14 \times WC + 0.27 \times AC - 0.18 \times CC + 0.29 \times TC \quad (13)$$

Units of years are used for age, kg for BM, and cm for height, WC, arm circumference (AC), calf circumference (CC) and thigh circumference (TC).

For males, the equations developed by Lee *et al.*, which correspond to equations 1–3 in the original report⁽⁴⁹⁾, are

$$BF\% = 44.47 + 0.10 \times \text{age} - 0.26 \times \text{height} + 0.29 \times BM \quad (14)$$

$$BF\% = 0.02 + 0.00 \times \text{age} - 0.07 \times \text{height} - 0.08 \times BM + 0.48 \times WC \quad (15)$$

$$BF\% = -3.10 + 0.01 \times \text{age} - 0.06 \times \text{height} - 0.10 \times BM + 0.49 \times WC - 0.09 \times AC - 0.02 \times CC + 0.12 \times TC \quad (16)$$

Fat-free mass characteristics

To provide a comprehensive examination of participant characteristics (Table 1) and confirm similarity with reference values, FFM characteristics were estimated using data from the aforementioned laboratory procedures. These characteristics included the density of FFM (D_{FFM}) and proportions of TBW, mineral (i.e. Mo + Ms) and residual (i.e. protein and glycogen) in FFM, designated as TBW:FFM, M:FFM and R:FFM. Residual

content (R) was calculated by subtraction using equation (17), with FM_{5C} representing the 5C model FM estimate:

$$R = BM - TBW - Mo - Ms - FM_{5C} \quad (17)$$

D_{FFM} , TBW:FFM, M:FFM, and F:FFM were calculated using equations (18–21), which are based on those presented by Wang *et al.*⁽⁵²⁾:

$$D_{FFM} = \frac{TBW + R + Mo + Ms}{\frac{TBW}{0.9937} + \frac{R}{1.34} + \frac{Mo}{2.982} + \frac{Ms}{3.317}} \quad (18)$$

$$TBW : FFM = TBW / FFM_{5C} \quad (19)$$

$$M : FFM = (Mo + Ms) / FFM_{5C} \quad (20)$$

$$R : FFM = R / FFM_{5C} \quad (21)$$

Statistical analysis

Sample size was determined based on resource availability due to the exploratory nature of this analysis; however, the final sample size was comparable with or larger than many previous validation studies^(10,13,24). Descriptive data for BF% estimates produced by each body composition model and method were generated (Table 3). The constant error (CE) was calculated as the mean difference between the 5C criterion and each alternate method (i.e. alternate estimate minus 5C estimate). Equivalence testing was used to evaluate whether each method demonstrated equivalence with the 5C model based on a 2% equivalence region, and the 90% confidence limits for the two-one-sided *t* tests were calculated⁽⁵³⁾. Null hypothesis significance testing (NHST) was also performed, and the 95% confidence limits were calculated. The Pearson correlation coefficient (*r*) and



Table 3. Body composition estimates*
(Mean values and standard deviations; 95 % confidence intervals)

Model	Body fat (%)				CE	95 % CI for CE (%)		P (NHST)	TE (%)	Equiv.	90 % TOST (%)		SEE rating†
	Mean	SD	Min	Max		LL	UL				LL	UL	
5C	26.2	8.8	8.9	46.7	–	–	–	–	–	–	–	–	–
4C	26.3	8.8	9.0	46.7	0.1	–0.1	0.0	<0.0001	0.1	Y	0.0	0.1	Ideal
4C _{MFBIA}	26.3	9.4	7.3	46.9	0.1	–0.4	0.3	0.73	2.1	Y	–0.2	0.3	Ideal
4C _{SFBIA}	27.3	8.7	9.9	47.6	1.0	–1.2	–0.9	<0.0001	1.6	Y	0.9	1.2	Ideal
4C _{DXA}	28.0	10.0	5.9	51.3	1.8	–2.1	–1.5	<0.0001	2.7	N	1.6	2.1	Ideal
3C	26.4	8.6	9.4	46.6	0.2	–0.3	–0.1	<0.0001	0.5	Y	0.2	0.3	Ideal
3C _{MFBIA}	26.4	9.2	7.9	46.8	0.2	–0.5	0.1	0.19	2.2	Y	–0.1	0.5	Ideal
3C _{SFBIA}	27.5	8.5	10.4	47.5	1.3	–1.6	–1.1	<0.0001	2.0	Y	1.1	1.5	Ideal
3C _{LOHMAN}	25.6	10.2	3.7	46.8	–0.6	0.2	1.0	0.002	2.7	Y	–1.0	–0.3	Ideal
DXA _{REG}	28.1	9.1	9.5	49.9	1.9	–2.2	–1.5	<0.0001	2.8	N	1.6	2.1	Ideal
DXA _{TISS}	29.1	9.3	9.9	51.3	2.9	–3.2	–2.6	<0.0001	3.6	N	2.6	3.2	Ideal
ADP _{BROZEK}	26.3	8.9	8.6	45.2	0.1	–0.5	0.2	0.46	2.3	Y	–0.2	0.4	Excellent
ADP _{SIRI}	27.1	9.5	8.0	47.6	0.9	–1.3	–0.5	<0.0001	2.6	Y	0.6	1.2	Ideal
BIS	26.0	8.4	8.4	47.5	–0.2	–0.2	0.6	0.3	2.4	Y	–0.5	0.1	Excellent
MFBIA	26.7	9.6	6.7	49.9	0.5	–1.0	0.0	0.03	3.1	Y	0.1	0.9	Very good
SFBIA	25.3	9.0	3.5	46.4	–0.9	0.4	1.4	0.0003	3.3	Y	–1.3	–0.5	Very good
DoD	25.6	9.6	1.7	50.9	–0.6	–1.4	0.2	0.16	5.4	Y	–1.3	0.1	Poor
LEE _{EQ1}	30.5	6.4	17.9	47.8	4.3	3.6	5.1	<0.0001	6.7	N	3.7	5.0	Poor
LEE _{EQ2}	31.8	6.9	19.4	50.4	5.6	4.9	6.3	<0.0001	7.3	N	5.0	6.2	Fair
LEE _{EQ3}	31.9	6.9	19.3	49.0	5.7	5.0	6.4	<0.0001	7.4	N	5.1	6.3	Fair

TOST, two one-sided test; CE, constant error; LL, lower limit of confidence interval; UL, upper limit of confidence interval; NHST, null hypothesis significance testing in the form of paired-samples *t* test. TE, total error; Equiv, equivalence testing result; SEE, standard error of the estimate; 5C, five-component model; 4C, four-component model; Y, yes, equivalent based on 2 % equivalence region; MFBIA, multi-frequency bioelectrical impedance analysis; SFBIA, single-frequency bioelectrical impedance analysis; DXA, dual-energy X-ray absorptiometry; N, no – not equivalent based on 2 % equivalence region; 3C, three-component model; REG, region; TISS, tissue; BROZEK, Brozek⁽³³⁾ two-component model body fat equation; SIRI, Siri⁽³²⁾ two-component model body fat equation; ADP, air displacement plethysmography; BIS, bioimpedance spectroscopy; DoD, Department of Defense body fat equation⁽⁴⁸⁾; LEE, Lee *et al.*⁽⁴⁹⁾ body fat equations.

* See Figs. 2–6 for additional validity metrics.

† Based on subjective ranking categories of Lohman & Milliken⁽⁵⁵⁾.

coefficient of determination (R^2) were estimated. Ordinary least squares and Deming regressions were performed to compare the intercept and slope of regression lines to the line of identity (i.e. the perfect linear relationship between methods with an intercept of 0 and a slope of 1). In contrast to ordinary least squares regression, which is commonly implemented in methodological investigations, Deming regression accounts for error in the measurement of both *x* and *y* variables and thus may be more appropriate when errors are present for both criterion and comparison methods⁽⁵⁴⁾. The standard error of the estimate (SEE; i.e. residual SE) was obtained from ordinary least squares regression. For both regression analyses, the 5C model was designated as the criterion variable (Y), and the alternate model was designated as the predictor variable (X). The subjective ranking categories of American College of Sports Medicine *et al.*⁽⁵⁵⁾ were utilised for categorisation of BF% SEE. The methods of Bland & Altman⁽⁵⁶⁾ were utilised alongside linear regression to assess the degree of proportional bias. The 95 % limits of agreement (LOA) were calculated. The total error (TE) (i.e. root mean square error or pure error) was calculated using equation (22):

$$TE = \sqrt{\frac{\sum(BF\%_{ALT} - BF\%_{5C})^2}{n}} \quad (22)$$

where $BF\%_{ALT}$ is the BF% estimate for the alternate body composition method in question. Data were analysed using R (version 3.6.1)⁽⁵⁷⁾. The primary packages utilised include *psych*⁽⁵⁸⁾, *TOSTER*⁽⁵⁹⁾, *deming*⁽⁵⁴⁾, *DescTools*⁽⁶⁰⁾ and *ggplot2*⁽⁶¹⁾.

Results

A broad summary of the performance of each method, including a comparison of CE, SEE and TE values, is displayed in Fig. 1.

Multi-component models

4C models exhibited CE values of 0.1–1.8 % and TE values of 0.1–2.7 % (Table 3). R^2 values ranged from 0.95 to 1.00, with SEE values of 0.02–1.99 % (Fig. 2). LOA ranged from 0.04 to 4.16 %. All 4C models except 4C_{DXA} demonstrated equivalence with 5C based on the 2 % equivalence interval.

3C models exhibited CE values of –0.6 to 1.3 % and TE values of 0.5–2.7 %. R^2 values ranged from 0.94 to 1.00, with SEE values of 0.39–2.10 % (Fig. 3). LOA ranged from 0.87 to 5.24 %, and all 3C models demonstrated equivalence with 5C (Table 3).

Laboratory methods

DXA BF% estimates exhibited CE values of 1.9–2.9 % and TE values of 2.8–3.6 % (Table 3). The R^2 value was 0.95 for both DXA BF% estimates, with SEE of approximately 2.1 % (Fig. 4). LOA ranged from 4.12 to 4.26 %, and neither DXA BF% estimate exhibited equivalence with 5C.

ADP BF% estimates exhibited CE values of 0.1–0.9 % and TE values of 2.3–2.6 % (Table 3). The R^2 value was 0.94 for both ADP BF% estimates, with SEE of approximately 2.2 % (Fig. 4). LOA ranged from 4.45 to 4.77 %, and both ADP BF% estimates exhibited equivalence with 5C.

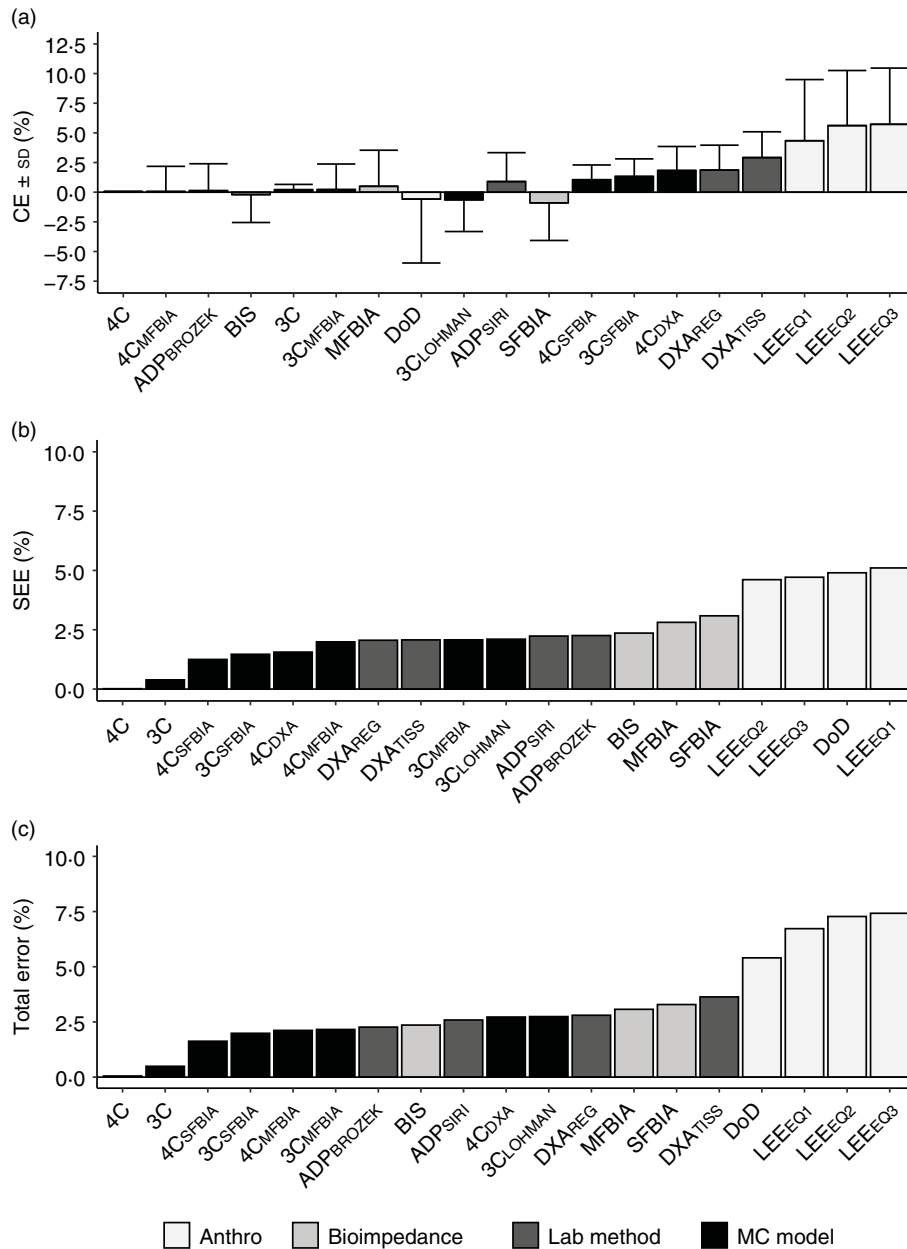


Fig. 1. Overview of select validity metrics. The constant error (CE; body fat % (BF%) for alternate method minus BF% value for 5C model) is displayed in panel (a). The standard error of the estimate (SEE; deviation of individual data points around the regression line) is displayed in panel (b). The TE (i.e. root mean square error or pure error; average deviation of individual scores from the line of identity) is displayed in panel (c). For all panels, methods are sorted in order of increasing error. 4C, four-component model; 5C, five-component model; ADP, air displacement plethysmography; BIS, bioimpedance spectroscopy; BROZEK, Brozek⁽³³⁾ two-component model body fat equation; CE, constant error; DoD, Department of Defense body fat equation⁽⁴⁸⁾; DXA, dual-energy X-ray absorptiometry; LEE, Lee *et al.*⁽⁴⁹⁾ body fat equations; MFBIA, multi-frequency bioelectrical impedance analysis; SFBIA, single-frequency bioelectrical impedance analysis; SIRI, Siri⁽³²⁾ two-component model body fat equation.

Field methods

Bioimpedance methods exhibited CE values of -0.9 to 0.5 % and TE values of 2.4–3.3 %. *R*² values ranged from 0.88 to 0.93, with SEE values of 2.36–3.09 % (Fig. 5). LOA ranged from 4.62 to 6.22 %, and all bioimpedance methods demonstrated equivalence with 5C (Table 3).

Anthropometric methods exhibited CE values of -0.6 to 5.7 % and TE values of 5.4–7.4 %. *R*² values ranged from 0.67 to 0.73,

with SEE values of 4.61–5.11 % (Fig. 6). LOA ranged from 9.10 to 10.56 %. Only the DoD BF% equation demonstrated equivalence with 5C (Table 3).

Discussion

The purpose of the present investigation was to determine the validity of body composition estimates from a variety of

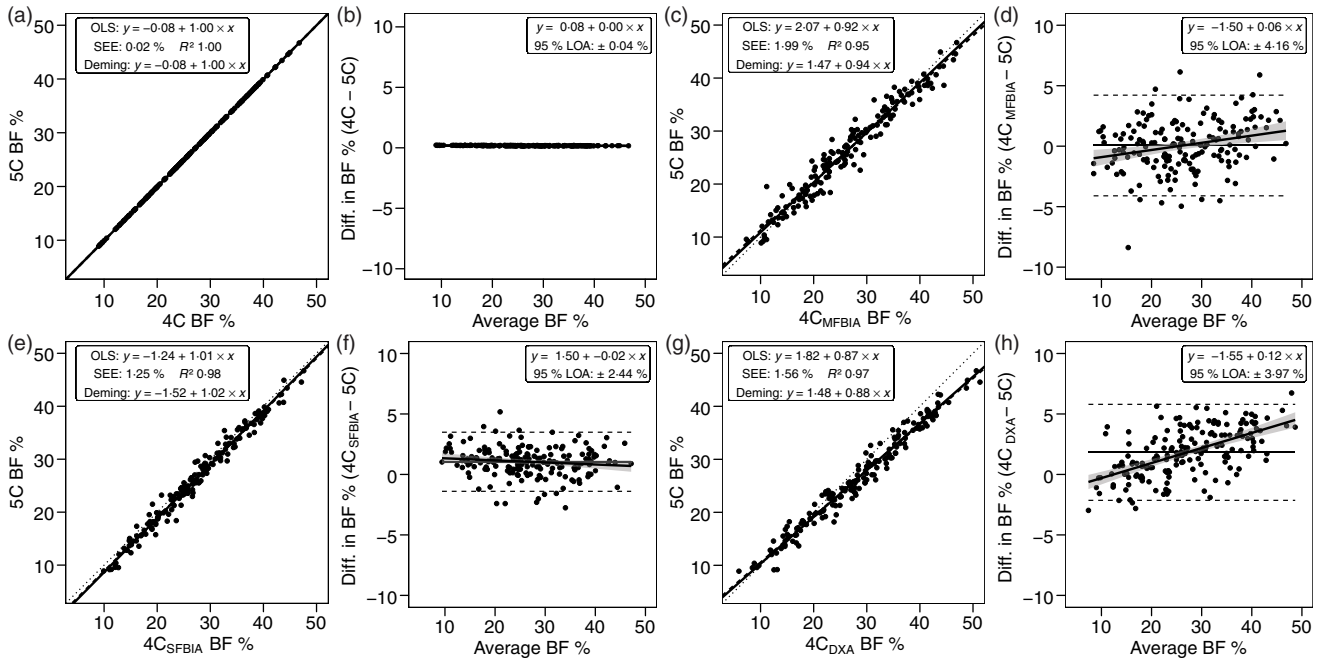


Fig. 2. Performance of four-component (4C) models. Validity analysis is displayed for 4C with BIS TBW estimates (a, b), 4C with multi-frequency BIA TBW estimates (c, d), 4C with SFBIA TBW estimates (e, f), and 4C with DXA-derived BV and BIS TBW estimates (g, h). The Wang *et al.*⁽⁸⁾ 4C equation was used for all models. Panels a, c, e and g depict ordinary least squares (OLS) regression lines (dashed) and Deming regression lines (solid) as compared with the line of identity (dotted). The standard error of the estimate (SEE) and coefficient of determination (R^2) are also displayed. Panels b, d, f and h depict Bland–Altman analysis, with the solid diagonal line representing the relationship between the difference in body composition estimates, calculated as the comparison method estimate minus the five-component (5C) estimate, and the average of comparison and 5C estimates. The shaded regions around the diagonal line indicate the 95% confidence limits for the linear regression line, the horizontal dashed lines indicate the upper and lower limits of agreement (LOA), and the horizontal solid line indicates the constant error between methods. Linear regression equations and 95% LOA values are also displayed. BIS, bioimpedance spectroscopy; TBW, total body water; SFBIA, single-frequency bioelectrical impedance analysis; DXA, dual-energy X-ray absorptiometry; BV, body volume; BF, body fat.

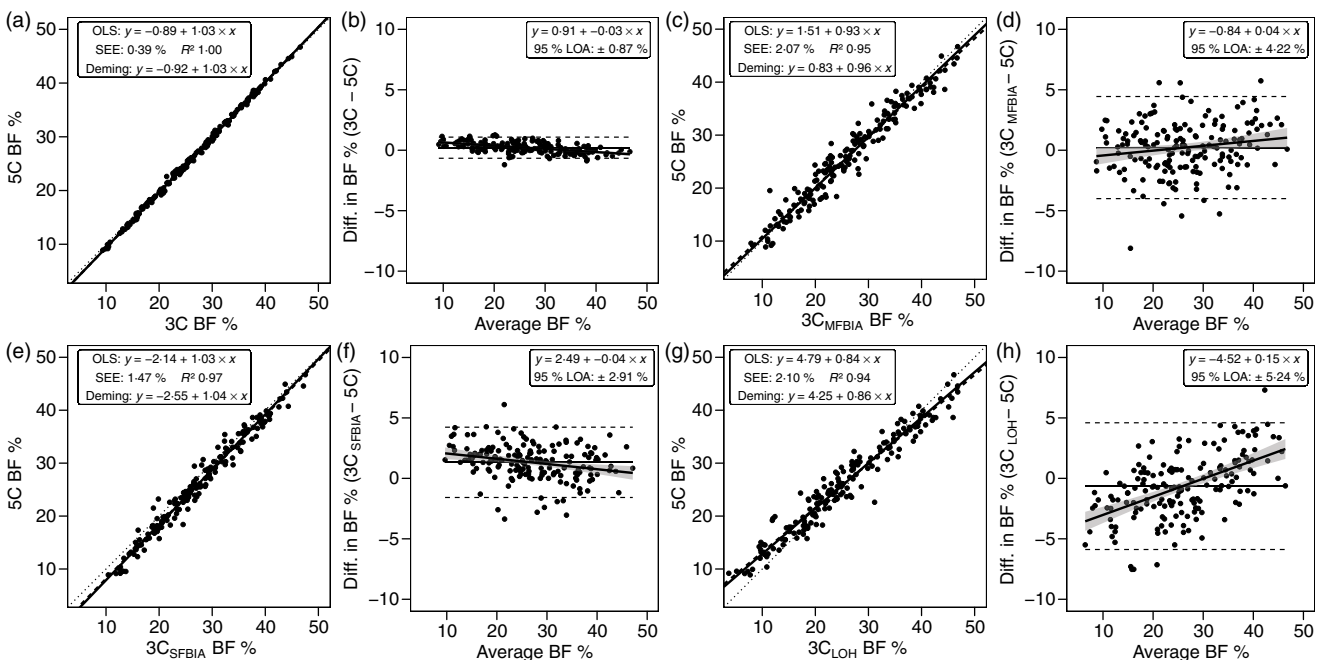


Fig. 3. Performance of three-component (3C) models. Validity analysis is displayed for Siri 3C model⁽⁴⁵⁾ with BIS TBW estimates (a, b), Siri 3C model with multi-frequency BIA TBW estimates (c, d), Siri 3C model with SFBIA TBW estimates (e, f), and Lohman 3C model⁽⁴⁶⁾ (g, h). Panels a, c, e and g depict ordinary least squares (OLS) regression lines (dashed) and Deming regression lines (solid) as compared with the line of identity (dotted). The standard error of the estimate (SEE) and coefficient of determination (R^2) are also displayed. Panels b, d, f and h depict Bland–Altman analysis, with the solid diagonal line representing the relationship between the difference in body composition estimates, calculated as the comparison method estimate minus the five-component (5C) estimate, and the average of comparison and 5C estimates. The shaded regions around the diagonal line indicate the 95% confidence limits for the linear regression line, the horizontal dashed lines indicate the upper and lower limits of agreement (LOA), and the horizontal solid line indicates the constant error between methods. Linear regression equations and 95% LOA values are also displayed. BIS, bioimpedance spectroscopy; TBW, total body water; SFBIA, single-frequency bioelectrical impedance analysis; BF, body fat.



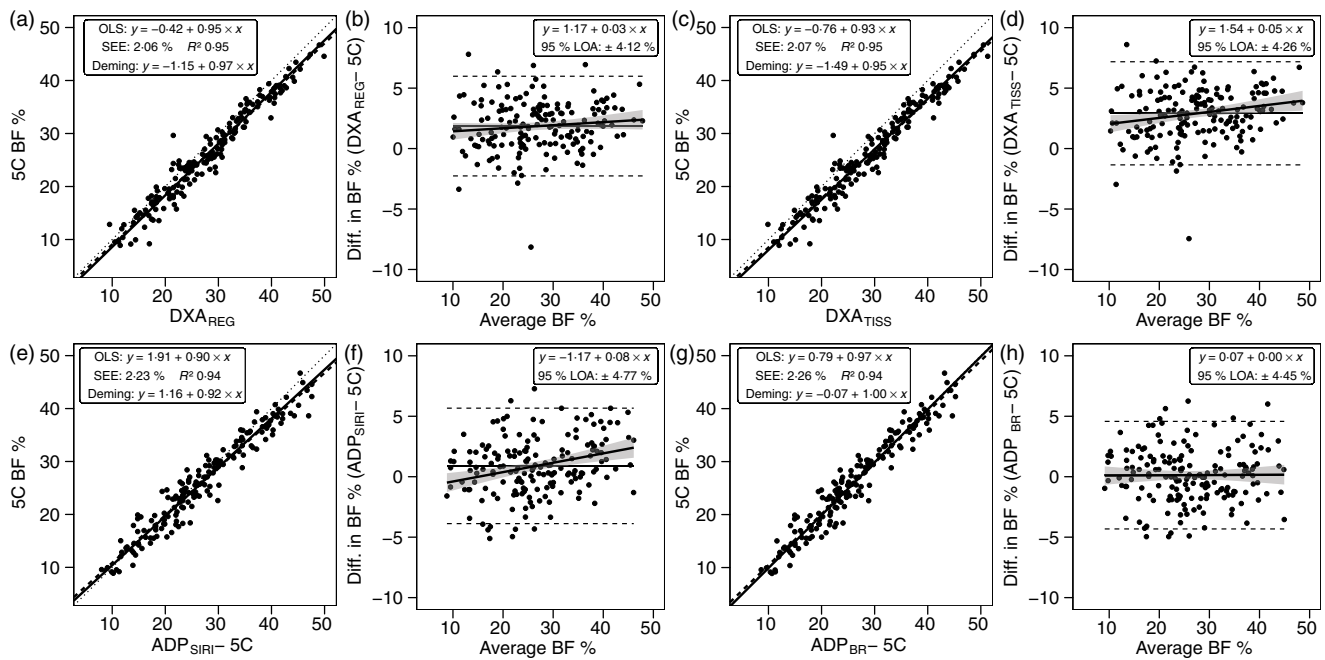


Fig. 4. Performance of dual-energy X-ray absorptiometry (DXA) and air displacement plethysmography (ADP). Validity analysis is displayed for DXA region body fat % (BF%) (a, b), DXA tissue BF% (c, d), ADP BF% with Siri equation⁽³²⁾ (e, f), and ADP BF% with Brozek equation⁽³³⁾ (g, h). Panels a, c, e and g depict ordinary least squares (OLS) regression lines (dashed) and Deming regression lines (solid) as compared with the line of identity (dotted). The standard error of the estimate (SEE) and coefficient of determination (R^2) are also displayed. Panels b, d, f and h depict Bland–Altman analysis, with the solid diagonal line representing the relationship between the difference in body composition estimates, calculated as the comparison method estimate minus the five-component (5C) estimate, and the average of comparison and 5C estimates. The shaded regions around the diagonal line indicate the 95% confidence limits for the linear regression line, the horizontal dashed lines indicate the upper and lower limits of agreement (LOA), and the horizontal solid line indicates the constant error between methods. Linear regression equations and 95% LOA values are also displayed.

commonly employed methods as compared with a 5C model criterion. Major findings were (1) differences between 5C, 4C and 3C models utilising the same BV and TBW estimates are negligible ($CE \leq 0.2\%$; $SEE < 0.5\%$; $TE \leq 0.5\%$; $R^2 \geq 1.00$; $95\% LOA \leq 0.9\%$), indicating that these models can be viewed interchangeably in many cases and that the utility of additional mineral estimates (i.e. bone mineral and soft tissue mineral) are questionable; (2) errors introduced by utilising alternate TBW (i.e. multi-frequency bioelectrical impedance analysis or SFBIA) or BV (i.e. DXA-derived) estimates are relatively small but would likely be meaningful in some contexts ($CE \leq 1.3\%$; $SEE \leq 2.1\%$; $TE \leq 2.2\%$; $R^2 \geq 0.95$; $95\% LOA \leq 4.2\%$); (3) small but potentially relevant differences between alternate DXA (i.e. tissue *v.* region) and ADP (i.e. Siri *v.* Brozek equations) BF% estimates were observed, and these techniques generally performed well ($CE < 3.0\%$; $SEE \leq 2.3\%$; $TE \leq 3.6\%$; $R^2 \geq 0.88$; $95\% LOA < 4.8\%$); (4) bioimpedance technologies performed relatively well ($CE < 1.0\%$; $SEE \leq 3.1\%$; $TE \leq 3.3\%$; $R^2 \geq 0.94$; $95\% LOA \leq 6.2\%$), although individual-level errors were generally larger than all other non-anthropometric methods and (5) newer anthropometric BF% equations produced using NHANES data did not outperform the DoD BF% equation and in fact exhibited much higher group-level error (DoD: $CE = 0.6\%$; NHANES: $CE = 4.3\text{--}5.7\%$); as expected, performance of anthropometric equations was relatively poor compared with other methods ($SEE \leq 5.1\%$; $TE \leq 7.4\%$; $R^2 \geq 0.67$; $95\% LOA \leq 10.6\%$). Importantly, the context in which a method is utilised and the

purpose of the assessment impact the interpretation of the observed errors. For example, while DXA demonstrated a statistically significant difference from 5C and lack of equivalence, both of which are group-level considerations, the SEE and 95% LOA, both of which provide information regarding individual-level validity, indicated relatively low error.

In contrast to the present study, several prior validity examinations of DXA as compared with a multi-component model have indicated an underestimation of BF% by DXA at the group level⁽¹⁰⁾. However, meaningful differences in DXA scanning and software technology limit the ability to compare results across studies with differing methodologies. In fact, although an earlier software version was used, prior research using the same DXA scanner as the present investigation (GE Lunar Prodigy) demonstrated overestimations of BF% relative to a 4C model that were very similar to those of the present study (1.7–2.3 *v.* 1.9%)⁽⁶²⁾. In the present analysis, it was also observed that the region BF% value, which is based on all observed pixels, exhibited slightly better agreement with 5C as compared with the tissue BF% value, which is based only on soft tissue pixels. The difference amounted to 1.0% on average (CE of 1.9 *v.* 2.9%) and resulted in a better TE value for DXA_{REGION} as compared with DXA_{TISSUE} (2.8 *v.* 3.6%). The closer agreement of the region BF% value is reasonable based on the fact that bone mineral is included in both the 5C and DXA_{REGION} , but not DXA_{TISSUE} . Based on examination of publicly available NHANES data, it was confirmed that the NHANES dataset, and therefore published

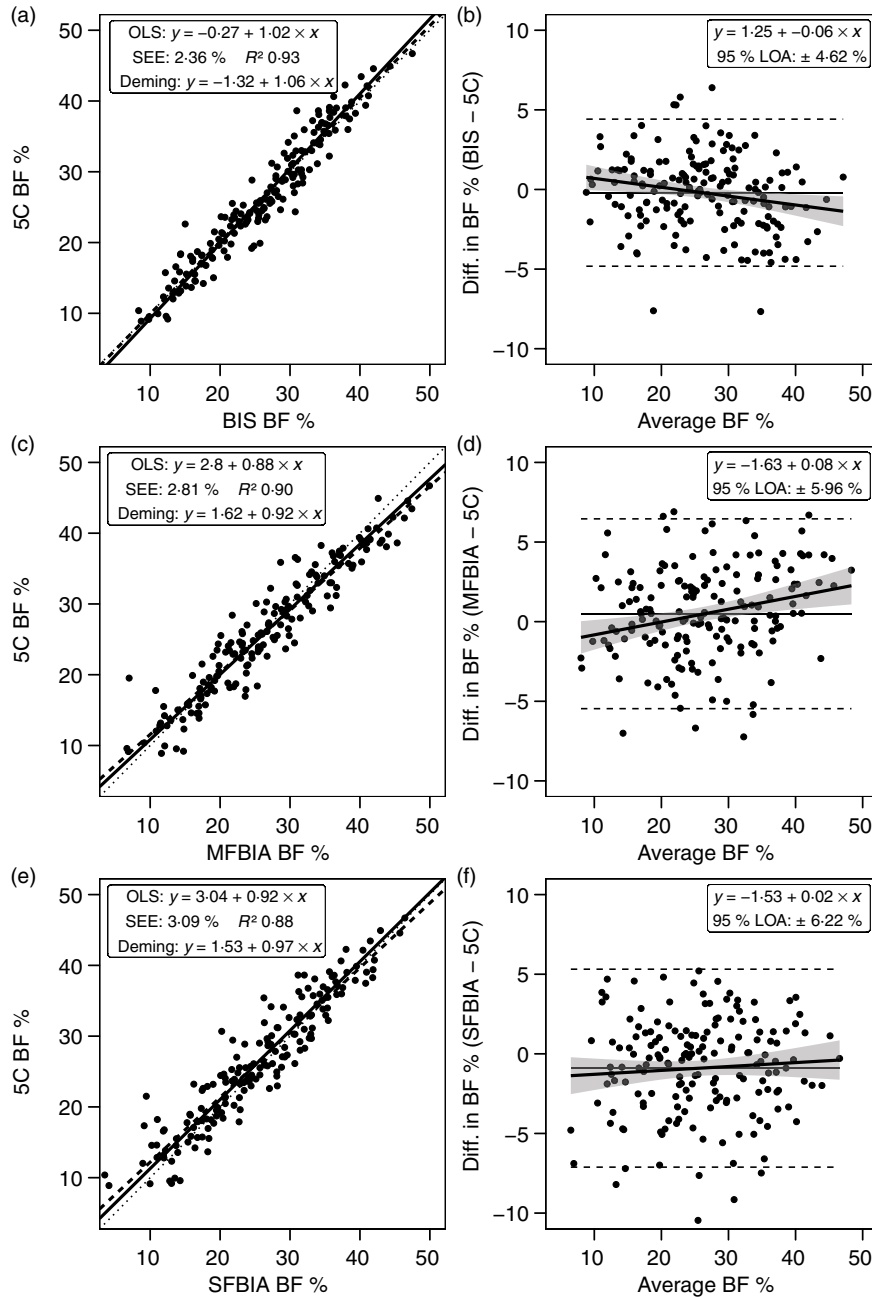


Fig. 5. Performance of bioimpedance techniques. Validity analysis is displayed for bioimpedance spectroscopy (BIS) (a, b), multi-frequency bioelectrical impedance analysis (MFBI) (c, d), and single-frequency bioelectrical impedance analysis (SFBI) (e, f). Panels a, c and e depict ordinary least squares (OLS) regression lines (dashed) and Deming regression lines (solid) as compared with the line of identity (dotted). The standard error of the estimate (SEE) and coefficient of determination (R^2) are also displayed. Panels b, d and f depict Bland–Altman analysis, with the solid diagonal line representing the relationship between the difference in body composition estimates, calculated as the comparison method estimate minus the five-component (5C) estimate, and the average of comparison and 5C estimates. The shaded regions around the diagonal line indicate the 95% confidence limits for the linear regression line, the horizontal dashed lines indicate the upper and lower limits of agreement (LOA), and the horizontal solid line indicates the constant error between methods. Linear regression equations and 95% LOA values are also displayed. BF, body fat.

reference values from this dataset⁽⁶³⁾, utilise region BF%. Based on calculation, the mean difference between region and tissue BF% in the 1999–2004 NHANES dataset is 1.0 (SD 0.2)%, with a higher estimate for tissue BF%. This difference of 1% is identical to that observed in the present investigation. In terms of practical application, personnel observing multiple BF% values on DXA reports should interpret and report the region BF% value for superior validity and better alignment with reference values.

For ADP, it was observed that the Brozek equation⁽³³⁾ slightly outperformed the Siri equation⁽³²⁾. Both of these are offered as options within the ADP software and are commonly utilised for BF% estimation^(24,64). ADP_{BROZEK} BF% did not differ from 5C based on NHST (CE: 0.1%; TE: 2.3%), unlike the ADP_{SIRI} BF% estimates (CE: 0.9%; TE: 2.6%). However, both methods demonstrated equivalence with 5C based on the 2% equivalence region. Additionally, the R^2 , SEE and LOA did not meaningfully

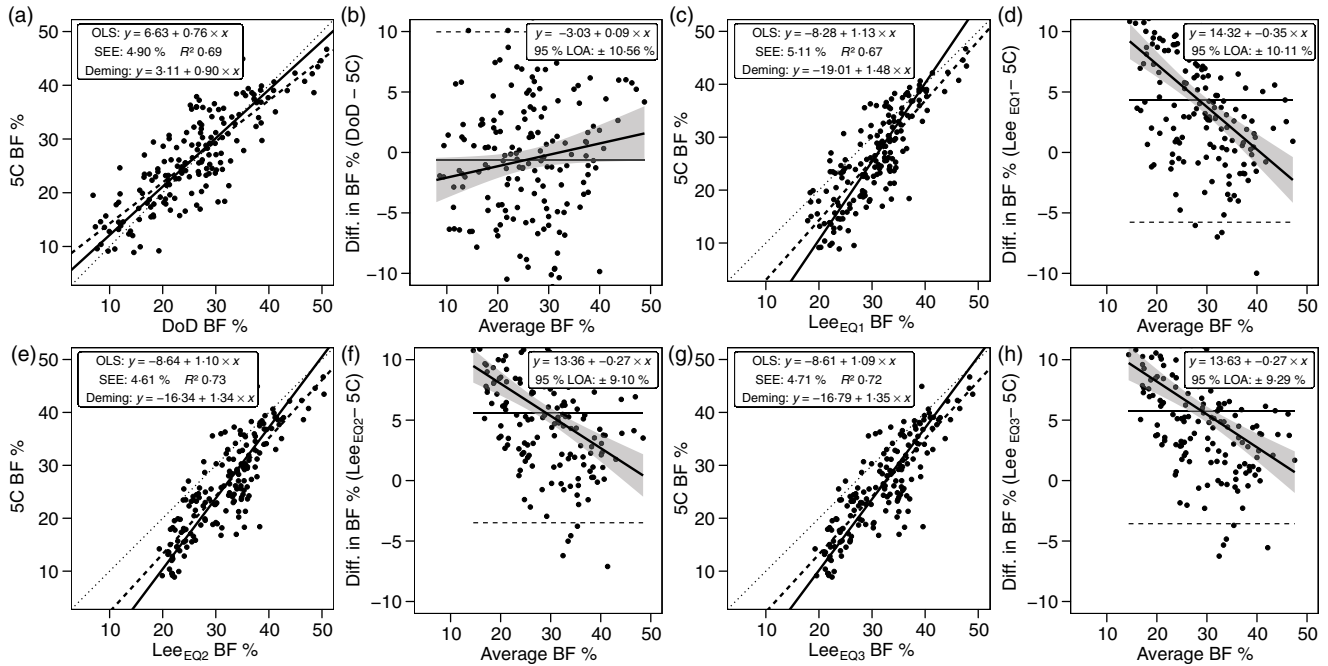


Fig. 6. Performance of anthropometric equations. Validity analysis is displayed for the Department of Defense (DoD) body fat % (BF%) equation⁽⁴⁸⁾ (a, b), Lee *et al.*⁽⁴⁹⁾ equation (1) (c, d), Lee *et al.*⁽⁴⁹⁾ equation (2) (e, f) and Lee *et al.*⁽⁴⁹⁾ equation (3) (g, h). Panels a, c, e and g depict ordinary least squares (OLS) regression lines (dashed) and Deming regression lines (solid) as compared with the line of identity (dotted). The standard error of the estimate (SEE) and coefficient of determination (R^2) are also displayed. Panels b, d, f and h depict Bland–Altman analysis, with the solid diagonal line representing the relationship between the difference in body composition estimates, calculated as the comparison method estimate minus the five-component (5C) estimate, and the average of comparison and 5C estimates. The shaded regions around the diagonal line indicate the 95% confidence limits for the linear regression line, the horizontal dashed lines indicate the upper and lower limits of agreement (LOA) and the horizontal solid line indicates the constant error between methods. Linear regression equations and 95% LOA values are also displayed.

differ between methods. However, ADP_{BROZEK} demonstrated a zero slope in the Bland–Altman analysis, indicative of no proportional bias, while ADP_{SIRI} had a slope of 0.08, indicative of larger overestimations of BF% in those with higher BF%. Several previous studies have indicated similar validity of ADP as compared with multi-component models⁽²⁴⁾. For example, Fields *et al.*⁽³¹⁾ demonstrated a TE of 2.3%, R^2 of 0.92 and SEE of 2.7% for BF% estimated by ADP, using the Siri equation, as compared with a molecular-level 4C model in adult females.

Bioimpedance technologies are widely available and frequently used for body composition estimation, although a series of assumptions and predictions are needed to traverse from the variables being assessed (i.e. raw bioelectrical properties of the body⁽⁶⁵⁾) to subsequent estimates of body composition^(66,67). One notable example is the ratio of TBW to FFM, which is typically assumed at approximately 0.73 despite meaningful variation between individuals (Table 1)^(68,69). While the substantial heterogeneity in commercially available bioimpedance devices and prediction equations makes broad conclusions regarding this technology more difficult, the present findings of low group-level errors (CE < 1.0%; $R^2 \geq 0.94$; equivalence with 5C) with somewhat poorer individual-level performance (95% LOA $\leq 6.2\%$) are consistent with prior research^(66,67).

Although anthropometric BF% estimates are rudimentary in comparison with many modern laboratory techniques, their simplicity and ease of implementation may contribute to their utility in some contexts⁽⁷⁰⁾. The DoD BF% equations, which utilise two

or three simple circumference estimates and height as input variables, have been a longstanding component of health and fitness assessments in the United States military^(25,48,71). Originally developed using hydrodensitometry as a criterion method, the DoD equations were subsequently revalidated using other methods, including multi-component models⁽²⁵⁾. More recently, efforts have been made to produce more advanced anthropometric BF% equations for use in the general population. Lee *et al.*⁽⁴⁹⁾ utilised NHANES data to produce a series of body composition prediction equations with varying complexity. Three of the four BF% equations, which utilised DXA as a criterion method during development, were examined in the present study. These equations required inputs of age, height and weight, along with circumference estimates. Interestingly, while select metrics were marginally better than the DoD equation, the overall performance of the DoD equation was superior. Specifically, the CE ($-0.6 v. \geq 4.3\%$) and TE ($5.4 v. \geq 6.7\%$) were lower for the DoD equation. Additionally, the DoD equation was the only anthropometric BF% equation to exhibit equivalence with 5C and also had the smallest degree of proportional bias in Bland–Altman analysis ($|\text{slope}|$ of $0.09 v. \geq 0.27$). However, the SEE and LOA, indicative of individual accuracy, were poor for all anthropometric BF% equations. It should be noted that, although the reliability of anthropometric estimates from three-dimensional optical scanners is generally high⁽⁴⁴⁾, the anthropometric equations evaluated in the present study were developed using manual rather than digital measurements.

Prior reports have indicated that digital anthropometric estimates may exhibit either superior⁽⁵⁰⁾ or inferior⁽⁵¹⁾ reliability as compared with manual measurements. Differences between manual and digital measurements could have influenced the observed results for anthropometric equations.

It is acknowledged that the close agreement between the criterion 5C model and several alternate methods, particularly other multi-component models or methods providing input variables for the 5C model, is directly related to the shared data in these equations (Table 2). However, while this should be considered when interpreting results from different models, these overlaps are functionally unavoidable given the methods used to construct molecular-level multi-component models⁽⁶⁾. Additionally, these comparisons provide meaningful applications regarding the tradeoff between complexity and accuracy. For example, it was clearly demonstrated that negligible differences existed between the criterion 5C, the 4C (Wang equation⁽⁸⁾) and 3C (Siri equation⁽⁴⁵⁾). These three models share BM, BV and TBW estimates, and the lack of meaningful difference in BF% estimates indicates that the addition of bone and soft tissue mineral estimates is largely unnecessary. The implications of this finding are meaningful as bone mineral estimates are provided by DXA, a relatively expensive technology with greater regulatory requirements than many other technologies due to the low dose of radiation⁽⁷²⁾. However, it should be noted that the importance of mineral estimates, particularly bone mineral, could be greater in scenarios in which deviation from expected values could be present, such as ageing or pathology, and in longitudinal monitoring in which changes in mineral are expected.

There are both strengths and limitations of the present work. A notable strength is the use of a multi-component model, rather than a single laboratory technique, as the criterion method. A limitation is the use of BIS for the TBW estimate rather than a dilution technique, despite data indicating the validity of bioimpedance for TBW estimation. While clearly unfeasible for use in most body composition assessment settings, dilution-based TBW estimates are an important component of method validation. Nonetheless, the present data allow for meaningful interpretation of the potential interchangeability of several bioimpedance TBW estimates and an alternate BV estimate, as well as the inclusion or exclusion of mineral estimates and examination of common laboratory and field techniques. Additionally, it should be noted that the FFM characteristics estimated using the present methods are similar to reference values based on direct cadaver analysis (see Table 1 and footnote), and results from several individual techniques were similar to those previously obtained using multi-component models with dilution-based TBW estimates^(24,31,62).

In summary, the present work examined the validity of a variety of contemporary body composition assessment techniques. The analysis confirms the validity of several multi-component model variants and indicates questionable necessity of models containing more than three components for group-level assessments. Further support for the utility of DXA and ADP as useful techniques was provided; however, these techniques are likely inappropriate for validation of other body composition methods, with the potential exception of DXA for segmental body

composition estimates. While group-level performance of bioimpedance techniques was strong, the individual-level errors may reduce their utility for monitoring individuals. Finally, newer anthropometric equations did not exhibit improved performance as compared with the longstanding DoD equation. Collectively, the information presented in this manuscript can aid researchers and clinicians in selecting an appropriate body composition assessment method and understanding the associated errors when compared with a criterion multi-component model.

Acknowledgements

The following individuals are acknowledged for their essential contributions to data collection: M. Lane Moore, Marqui Benavides, Jacob Dellinger and Brian Adamson. The following individuals are acknowledged for their contributions to intellectual discussions related to the study: Jordan Moon, Zad Rafi and Nelson Griffiths.

No funding was received for this study. Several of the body composition assessment devices evaluated in the present study were donated or loaned by the manufacturers. The single-frequency bioelectrical impedance analyser was provided by RJL Systems (Clinton Township, MI, USA), and the three-dimensional optical scanner was provided by Size Stream® (Cary, NC, USA; Contract no. C12496). These entities had no role in the design, analysis or writing of this article.

G. M. T. was responsible for all aspects of the present work, with assistance in data collection from the individuals specified in the acknowledgements.

The author has received in-kind support in the form of product loan or donation from several companies that produce body composition assessment devices, including Size Stream LLC, Naked Labs Inc., RJL Systems, MuscleSound and Biospace Inc. (DBA InBody). The author declares no other potential conflicts of interest.

References

1. Gupta P, Lanca C, Gan ATL, *et al.* (2019) The association between body composition using dual energy X-ray absorptiometry and type-2 diabetes: a systematic review and meta-analysis of observational studies. *Sci Rep* **9**, 12634.
2. Gonzalez MC, Correia M & Heymsfield SB (2017) A requiem for BMI in the clinical setting. *Curr Opin Clin Nutr Metab Care* **20**, 314–321.
3. Santanasto AJ, Goodpaster BH, Kritchevsky SB, *et al.* (2017) Body composition remodeling and mortality: the health aging and body composition study. *J Gerontol A Biol Sci Med Sci* **72**, 513–519.
4. Zong G, Zhang Z, Yang Q, *et al.* (2016) Total and regional adiposity measured by dual-energy X-ray absorptiometry and mortality in NHANES 1999–2006. *Obesity* **24**, 2414–2421.
5. Ward LC (2018) Human body composition: yesterday, today, and tomorrow. *Eur J Clin Nutr* **72**, 1201–1207.
6. Heymsfield SB, Ebbeling CB, Zheng J, *et al.* (2015) Multi-component molecular-level body composition reference methods: evolving concepts and future directions. *Obes Rev* **16**, 282–294.



7. Wang ZM, Deurenberg P, Guo SS, *et al.* (1998) Six-compartment body composition model: inter-method comparisons of total body fat measurement. *Int J Obes Relat Metab Disord* **22**, 329–337.
8. Wang Z, Pi-Sunyer FX, Kotler DP, *et al.* (2002) Multicomponent methods: evaluation of new and traditional soft tissue mineral models by in vivo neutron activation analysis. *Am J Clin Nutr* **76**, 968–974.
9. Heymsfield SB, Lichtman S, Baumgartner RN, *et al.* (1990) Body composition of humans: comparison of two improved four-compartment models that differ in expense, technical complexity, and radiation exposure. *Am J Clin Nutr* **52**, 52–58.
10. Toombs RJ, Ducher G, Shepherd JA, *et al.* (2012) The impact of recent technological advances on the trueness and precision of DXA to assess body composition. *Obesity* **20**, 30–39.
11. Earthman C, Traugher D, Dobratz J, *et al.* (2007) Bioimpedance spectroscopy for clinical assessment of fluid distribution and body cell mass. *Nutr Clin Pract* **22**, 389–405.
12. Kyle UG, Bosaeus I, De Lorenzo AD, *et al.* (2004) Bioelectrical impedance analysis—part I: review of principles and methods. *Clin Nutr* **23**, 1226–1243.
13. Kyle UG, Bosaeus I, De Lorenzo AD, *et al.* (2004) Bioelectrical impedance analysis—part II: utilization in clinical practice. *Clin Nutr* **23**, 1430–1453.
14. Buendia R, Seoane F, Lindecrantz K, *et al.* (2015) Estimation of body fluids with bioimpedance spectroscopy: state of the art methods and proposal of novel methods. *Physiol Meas* **36**, 2171–2187.
15. Armstrong LE, Kenefick RW, Castellani JW, *et al.* (1997) Bioimpedance spectroscopy technique: intra-, extracellular, and total body water. *Med Sci Sports Exerc* **29**, 1657–1663.
16. Smith-Ryan AE, Mock MG, Ryan ED, *et al.* (2017) Validity and reliability of a 4-compartment body composition model using dual energy X-ray absorptiometry-derived body volume. *Clin Nutr* **36**, 825–830.
17. Wilson JP, Fan B & Shepherd JA (2013) Total and regional body volumes derived from dual-energy X-ray absorptiometry output. *J Clin Densitom* **16**, 368–373.
18. Wilson JP, Strauss BJ, Fan B, *et al.* (2013) Improved 4-compartment body-composition model for a clinically accessible measure of total body protein. *Am J Clin Nutr* **97**, 497–504.
19. Blue MNM, Hirsch KR, Trexler ET, *et al.* (2018) Validity of the 4-compartment model using dual energy X-ray absorptiometry-derived body volume in overweight individuals. *Appl Physiol Nutr Metab* **43**, 742–746.
20. Ng BK, Liu YE, Wang W, *et al.* (2018) Validation of rapid 4-component body composition assessment with the use of dual-energy X-ray absorptiometry and bioelectrical impedance analysis. *Am J Clin Nutr* **108**, 708–715.
21. Nickerson BS, Esco MR, Bishop PA, *et al.* (2017) Validity of four-compartment model body fat in physically active men and women when using DXA for body volume. *Int J Sport Nutr Exerc Metab* **27**, 520–527.
22. Nickerson BS, Fedewa MV, McLester CN, *et al.* (2020) Development of a dual-energy X-ray absorptiometry-derived body volume equation in Hispanic adults for administering a four-compartment model. *Br J Nutr* **123**, 1373–1381.
23. Tinsley GM (2018) Reliability and agreement between DXA-derived body volumes and their usage in 4-compartment body composition models produced from DXA and BIA values. *J Sports Sci* **36**, 1235–1240.
24. Fields DA, Goran MI & McCrory MA (2002) Body-composition assessment via air-displacement plethysmography in adults and children: a review. *Am J Clin Nutr* **75**, 453–467.
25. Friedl KE (2012) Body composition and military performance – many things to many people. *J Strength Cond Res* **26**, Suppl. 2, S87–S100.
26. Nana A, Slater GJ, Hopkins WG, *et al.* (2012) Effects of daily activities on dual-energy X-ray absorptiometry measurements of body composition in active people. *Med Sci Sports Exerc* **44**, 180–189.
27. Moore ML, Benavides ML, Dellinger JR, *et al.* (2020) Segmental body composition evaluation by bioelectrical impedance analysis and dual-energy X-ray absorptiometry: quantifying agreement between methods. *Clin Nutr* **39**, 2802–2810.
28. Tinsley GM, Moore ML & Graybeal AJ (2018) Precision of dual-energy X-ray absorptiometry reflection scans in muscular athletes. *J Clin Densitom* (Epublication ahead of print version 13 September 2018).
29. Hangartner TN, Warner S, Braillon P, *et al.* (2013) The Official Positions of the International Society for Clinical Densitometry: acquisition of dual-energy X-ray absorptiometry body composition and considerations regarding analysis and repeatability of measures. *J Clin Densitom* **16**, 520–536.
30. Millard-Stafford ML, Collins MA, Evans EM, *et al.* (2001) Use of air displacement plethysmography for estimating body fat in a four-component model. *Med Sci Sports Exerc* **33**, 1311–1317.
31. Fields DA, Wilson GD, Gladden LB, *et al.* (2001) Comparison of the BOD POD with the four-compartment model in adult females. *Med Sci Sports Exerc* **33**, 1605–1610.
32. Siri WE (1956) The gross composition of the body. *Adv Biol Med Phys* **4**, 239–280.
33. Brozek J, Grande F, Anderson JT, *et al.* (1963) Densitometric analysis of body composition: revision of some quantitative assumptions. *Ann N Y Acad Sci* **110**, 113–140.
34. Schutte JE, Townsend EJ, Hugg J, *et al.* (1984) Density of lean body mass is greater in blacks than in whites. *J Appl Physiol* **56**, 1647–1649.
35. Ortiz O, Russell M, Daley TL, *et al.* (1992) Differences in skeletal muscle and bone mineral mass between black and white females and their relevance to estimates of body composition. *Am J Clin Nutr* **55**, 8–13.
36. Moon JR, Tobkin SE, Roberts MD, *et al.* (2008) Total body water estimations in healthy men and women using bioimpedance spectroscopy: a deuterium oxide comparison. *Nutr Metab* **5**, 7.
37. Moon JR, Smith AE, Tobkin SE, *et al.* (2009) Total body water changes after an exercise intervention tracked using bioimpedance spectroscopy: a deuterium oxide comparison. *Clin Nutr* **28**, 516–525.
38. Tinsley GM, Moore ML, Benavides ML, *et al.* (2020) 3-Dimensional optical scanning for body composition assessment: a 4-component model comparison of four commercially available scanners. *Clin Nutr* **39**, 3160–3167.
39. Cole KS (1940) Permeability and impermeability of cell membranes for ions. *Cold Spring Harb Symp Quant Biol* **8**, 110–122.
40. Hanai T (1968) Electrical properties of emulsions. *Emulsion Sci*, 354–477.
41. Wang ZM, Xavier P-S, Kotler DP, *et al.* (2002) Multicomponent methods: evaluation of new and traditional soft tissue mineral models by in vivo neutron activation analysis. *Am J Clin Nutr* **76**, 968–974.
42. Bony-Westphal A, Schautz B, Later W, *et al.* (2013) What makes a BIA equation unique? Validity of eight-electrode multifrequency BIA to estimate body composition in a healthy adult population. *Eur J Clin Nutr* **67**, Suppl. 1, S14–S21.
43. co. Sg (2016) seca 515/514 Product Manual v. 1.1.
44. Tinsley GM, Moore ML, Dellinger JR, *et al.* (2020) Digital anthropometry via three-dimensional optical scanning:

- evaluation of four commercially available systems. *Eur J Clin Nutr* **74**, 1054–1064.
45. Siri WE (1961) Body composition from fluid spaces and density: analysis of methods. In *Techniques for Measuring Body Composition*, pp. 223–244 [A Henschel and J Brožek, editors]. Washington, DC: National Academy of Sciences/National Research Council.
 46. Lohman TG (1986) 11 Applicability of body composition techniques and constants for children and youths. *Exerc Sport Sci Rev* **14**, 325–357.
 47. Moon JR, Eckerson JM, Tobkin SE, *et al.* (2009) Estimating body fat in NCAA Division I female athletes: a five-compartment model validation of laboratory methods. *Eur J Appl Physiol* **105**, 119–130.
 48. United States Government US Army (2019) *Army Regulation 600-9: The Army Body Composition Program*.
 49. Lee DH, Keum N, Hu FB, *et al.* (2017) Development and validation of anthropometric prediction equations for lean body mass, fat mass and percent fat in adults using the National Health and Nutrition Examination Survey (NHANES) 1999–2006. *Br J Nutr* **118**, 858–866.
 50. Medina-Inojosa J, Somers VK, Ngwa T, *et al.* (2016) Reliability of a 3D body scanner for anthropometric measurements of central obesity. *Obes Open Access* **2**.
 51. Bourgeois B, Ng BK, Latimer D, *et al.* (2017) Clinically applicable optical imaging technology for body size and shape analysis: comparison of systems differing in design. *Eur J Clin Nutr* **71**, 1329–1335.
 52. Wang Z, Heshka S, Wang J, *et al.* (2003) Magnitude and variation of fat-free mass density: a cellular-level body composition modeling study. *Am J Physiol Endocrinol Metab* **284**, E267–E273.
 53. Dixon PM, Saint-Maurice PF, Kim Y, *et al.* (2018) A primer on the use of equivalence testing for evaluating measurement agreement. *Med Sci Sports Exerc* **50**, 837–845.
 54. Therneau T (2018) deming: Deming, Theil-Sen, Passing-Bablok and Total Least Squares Regression.
 55. American College of Sports Medicine, Lohman TG & Milliken LA (2020) *ACSM's Body Composition Assessment*. Champaign, IL: Human Kinetics.
 56. Bland JM & Altman DG (1986) Statistical methods for assessing agreement between two methods of clinical measurement. *Lancet* **i**, 307–310.
 57. R Core Team (2019) *R: A Language and Environment for Statistical Computing*. Vienna: R Foundation for Statistical Computing.
 58. Revelle W (2019) *psych: Procedures for Psychological, Psychometric, and Personality Research*. Evanston, IL: Northwestern University.
 59. Lakens D (2017) Equivalence tests: a practical primer for *t*-tests, correlations, and meta-analyses. *Soc Psychol Personal Sci* **1**, 1–8.
 60. al ASem (2019) DescTools: Tools for Descriptive Statistics.
 61. Wickham H (2016) *ggplot2: Elegant Graphics for Data Analysis*. New York: Springer-Verlag.
 62. Williams JE, Wells JC, Wilson CM, *et al.* (2006) Evaluation of Lunar Prodigy dual-energy X-ray absorptiometry for assessing body composition in healthy persons and patients by comparison with the criterion 4-component model. *Am J Clin Nutr* **83**, 1047–1054.
 63. Kelly TL, Wilson KE & Heymsfield SB (2009) Dual energy X-ray absorptiometry body composition reference values from NHANES. *PLoS ONE* **4**, e7038.
 64. Fedewa MV, Nickerson BS, Tinsley GM, *et al.* (2019) Examining race-related error in two-compartment models of body composition assessment: a systematic review and meta-analysis. *J Clin Densitom* (Epublication ahead of print version 30 October 2019).
 65. Tinsley GM, Moore ML, Silva AM, *et al.* (2020) Cross-sectional and longitudinal agreement between two multifrequency bioimpedance devices for resistance, reactance, and phase angle values. *Eur J Clin Nutr* **74**, 900–911.
 66. Ward LC (2019) Bioelectrical impedance analysis for body composition assessment: reflections on accuracy, clinical utility, and standardisation. *Eur J Clin Nutr* **73**, 194–199.
 67. Moon JR (2013) Body composition in athletes and sports nutrition: an examination of the bioimpedance analysis technique. *Eur J Clin Nutr* **67**, Suppl. 1, S54–S59.
 68. Tinsley GM, Graybeal AJ, Moore ML, *et al.* (2019) Fat-free mass characteristics of muscular physique athletes. *Med Sci Sports Exerc* **51**, 193–201.
 69. Wang Z, Deurenberg P, Wang W, *et al.* (1999) Hydration of fat-free body mass: review and critique of a classic body-composition constant. *Am J Clin Nutr* **69**, 833–841.
 70. Flegal KM, Shepherd JA, Looker AC, *et al.* (2009) Comparisons of percentage body fat, body mass index, waist circumference, and waist-stature ratio in adults. *Am J Clin Nutr* **89**, 500–508.
 71. Hodgdon JA & Friedl KE (1999) Technical Document No. 99-2B: Development of the DoD Body Composition Estimation Equations.
 72. Shepherd JA, Ng BK, Sommer MJ, *et al.* (2017) Body composition by DXA. *Bone* **104**, 101–105.